Thus S is very much smaller for (d,α) reactions leading to states of type (b) for which n is odd, than for those leading to states of type (a) for which n is even. For example, for $j=5/2$, $n=3$ gives $S=0.67$ whereas $n=4$ gives $S=4.0$. Thus, peak A is larger than peak B by a factor of $4\times4.0/0.67$ (the first factor of 4 is from the number of levels, considered above) $=24$. Thus it is not surprising that only peak A is prominent in the experimental results, and the spectra are very similar for odd- and even-mass nuclei.

V. CONCLUSION

Of the two strong alpha-particle groups observed in the energy spectra, the low-energy peak was found to be predominantly a compound-nucleus evaporation effect and to be in good agreement with the predictions of statistical theory. The principal features of the high-energy peak can be explained by a two-particle pickup process which involves the removal of nucleons from combinations of single-particle states in the filling major shells.

There are, however, additional features of the energy distributions that cannot be easily explained. For instance, the triple peak observed in Pr and Nd. These peaks are not the result of a mixture of isotopes, since Pr is mono-isotopic. A tendency towards double peaking in the energy spectra is also apparent for the elements Er and Te. These features appear to be isolated parts of a systematic trend for these regions. At the time of data accumulation, few targets were available for these ranges of nuclei, and large intervals in atomic number could not be studied.

A more thorough understanding of the nature of the high-energy peak can only be obtained with higher resolution experiments. At present such a program is under way utilizing diffused junction solid-state detectors and mono-isotopic targets. The results of this study will be presented in a forthcoming article.

ACKNOWLEDGMENTS

The authors wish to express their appreciation to Dr. Elizabeth Baranger, Dr. Karl Quisenberry and Dr. Allen G. Blair for helpful discussions and suggestion concerning certain phases of this work. They are indebted to William Stewart and John DeFrancesco for invaluable assistance in making calculations and in the collection and processing of data. They wish to thank the members of the cyclotron staff and machine shop personnel for their cooperation. Special thanks are due Mr. George Fodor for preparing and mounting most of the targets used in this experiment and to Mr. Johannes Bakker for his assistance in solving many electronics problems.

The authors also wish to thank Dr. A. J. Allen and acknowledge the financial support given by the joint program of the Office of Naval Research and the U. S. Atomic Energy Commission and by the National Science Foundation.

PHYSICAL REVIEW VOLUME 125, NUMBER 3 FEBRUARY 1, 1962

Neutron Giant Resonances—Nuclear Ramsauer Effect*

J. M. PETERSON
Lawrence Radiation Laboratory, University of California, Livermore, California and Institute for Theoretical Physics, Copenhagen, Denmark

(Received July 31, 1961)

Three continuous families of broad maxima and minima are observed in neutron total cross sections between 0.1 and 100 Mev. All shift smoothly to higher energy with increasing mass number. The relationships among the families, their energy-mass number dependence, and their detailed locations can be understood in terms of a semiclassical treatment of a simplified optical model. The oscillations are seen to result from interference between the part of the neutron wave which has traversed the nucleus with the part which has gone around. This nuclear situation is analogous to the Ramsauer effect in electron interactions with noble gases. An alternative explanation of the broad maxima as due to resonances of single partial waves is not valid because in general several partial waves are simultaneously important and because the partial wave characteristics change rapidly as one traverses a continuous family of maxima. The widths of the broad maxima are related more to the parameters of the real potential well than to the depth of the imaginary potential well.

I. INTRODUCTION

THE curves of neutron total cross section versus energy often show broad maxima in the energy region of a few Mev and higher. These maxima are illustrated in Fig. 1. Before the measurements were made it had been expected on theoretical grounds that the variation with energy would be a simple monotonic decrease—something like $2\pi(R+\lambda\!\!\!^{-})^2$, R being the nuclear radius and $\lambda\!\!\!^{-}$ the neutron wavelength divided by 2π. The theoretical model[1] here was that the nucleus was black to neutrons. Note that on the average this model gave

* The work described in this report was initiated at the Lawrence Radiation Laboratory, University of California, and completed in its final form at the Institute for Theoretical Physics, Copenhagen, Denmark. It was supported by the U. S. Atomic Energy Commission.

[1] H. Feshbach and V. F. Weisskopf, Phys. Rev. **76**, 1550 (1949).

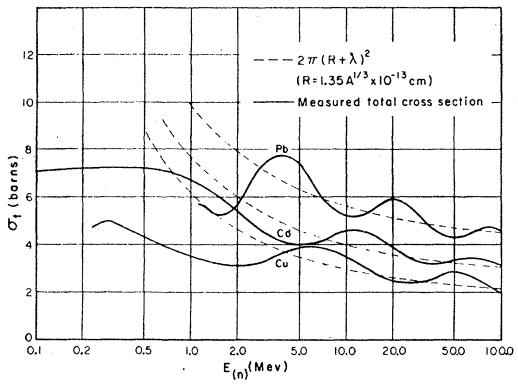

FIG. 1. Measured neutron total cross sections for lead, cadmium, and copper as functions of neutron energy, which show typical neutron giant resonances.

the correct cross section, although it did not account for the oscillations, whose amplitudes amount to as much as 25% of the average values at low energies and are typically 10% at the higher energies.

These giant resonances were first observed and pointed out by Barschall[2] and co-workers at the University of Wisconsin, who made systematic measurements up to 3 Mev. Many other sets of measurements[3] have been made, notable ones being those of Nereson and Darden[4] at Los Alamos, who measured from 3 to 13 Mev, those of Coon *et al.*[5] at Los Alamos at 14 Mev, and those of Taylor and Wood[6] at Harwell from 30 to 150 Mev. More recently Bratenahl *et al.*[7] at Livermore have measured a large number of elements over the range 7 to 30 Mev, and Bowen *et. al.*[8] at Harwell have measured a series between 16 and 118 Mev.

Altogether these total cross-section data, plotted against both energy E and mass number A, form a smooth surface in which three continuous ridges of giant resonances are apparent. Figure 2 is a three-dimensional, Barschall-type plot covering the neutron energy range from 1 to 30 Mev; on this plot two of the ridges and a hint of a third at higher energies can be seen. The positions $(E,A^{\frac{1}{3}})$ of all the broad maxima and minima which have been experimentally observed for neutron energies up to 100 Mev are plotted in Fig. 3. Note that just three families of maxima (and minima) occur and that they all seem intimately related somehow. (There is another group of broad maxima, all of which occur at about 1.5 or 2.0 Bev, but they arise from meson effects, presumably, and will be ignored in this discussion.) Note too that the slope of the locus of each family is everywhere *positive* in the E, $A^{\frac{1}{3}}$ plane.

These data have been explained theoretically by various optical-model calculations with varying degrees of success. In this type of model the neutron-nucleus interaction is represented by a complex potential well. The best known of these representations is that of Feshbach *et al.*,[9] who fitted their model to the 0- to 3-Mev data of Barschall and co-workers. This model was particularly successful in the low-energy region; at thermal energies it explained the peaks in the strength function distribution[9,10] and the discontinuities in the scattering length distribution[11] near $A=55$ and $A=155$ ($A^{\frac{1}{3}}=3.8$ and 5.4, respectively) as due to resonances of s waves. The resonant condition for low-energy s-wave resonances in a square potential well is that there be an integral number of half-wavelengths inside the nucleus, i.e., that $k_{\text{in}}R=(m+\frac{1}{2})\pi$, where k_{in} is the neutron wave number inside the nucleus of radius R, and m is any integer. The model predicted, furthermore, that p-wave resonances should occur near $A=25$ and $A=90$ ($A^{\frac{1}{3}}=2.9$ and 4.5, respectively), where $k_{\text{in}}R=m\pi$. This prediction was substantiated by Newson and co-workers[12] working in the energy region 30 to 110 kev, who observed peaks

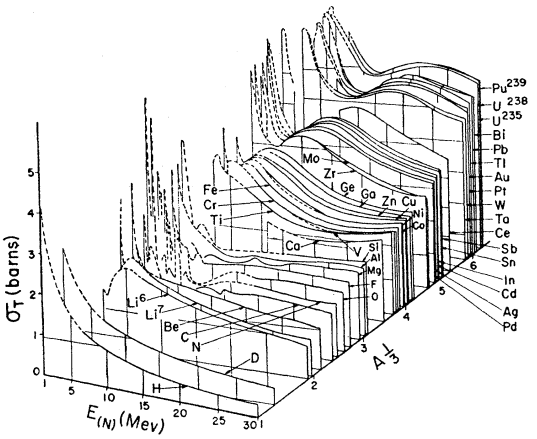

FIG. 2. Three-dimensional plot of measured neutron total cross sections versus neutron energy and versus $A^{\frac{1}{3}}$, covering the energy range 1 to 30 Mev. Continuous families of broad maxima are exhibited.

[2] H. H. Barschall, Phys. Rev. **86**, 431 (1952).

[3] See references in compilation *Neutron Cross Sections*, Second edition, compiled by D. J. Hughes and R. Schwartz, Brookhaven National Laboratory Report BNL-325 (Superintendent of Documents, U. S. Government Printing Office, Washington, D. C., 1958), and Suppl.

[4] N. Nereson and S. E. Darden, Phys. Rev. **89**, 775 (1953): **94**, 1682 (1954).

[5] J. H. Coon, E. R. Graves, and H. H. Barschall, Phys. Rev. **88**, 562 (1952).

[6] A. E. Taylor and E. Wood, Phil. Mag. **44**, 95 (1953).

[7] A. Bratenahl, J. M. Peterson, and J. P. Stoering, Phys. Rev. **110**, 927 (1958): **120**, 521 (1960).

[8] P. H. Bowen, J. P. Scanlon, G. H. Stafford, J. J. Thresher, and P. E. Hodgson, Nuclear Phys. **22**, 640 (1961).

[9] H. Feshbach, C. E. Porter, and V. F. Weisskopf, Phys. Rev. **90**, 166 (1953): **96**, 448 (1954). Also, X. Campbell, H. Feshbach, C. E. Porter, and V. F. Weisskopf, Massachusetts Institute of Technology Laboratory Nuclear Science Technical Report 73, 1960 (unpublished).

[10] V. F. Weisskopf, Revs. Modern Phys. **29**, 174 (1957): D. M. Chase, L. Wilets, and A. R. Edmonds, Phys. Rev. **110**, 1080 (1958).

[11] K. W. Ford and D. Bohm, Phys. Rev. **79**, 746 (1950): R. K. Adair, *ibid.* **94**, 737 (1954).

[12] R. C. Block, W. Haeberli, and H. W. Newson, Phys. Rev. **109**, 1620 (1958): H. W. Newson, R. C. Block, P. F. Nichols, A. Taylor, A. K. Furr, and E. Merzbacher, Ann. Phys. **8**, 211 (1959).

near $A=25$ and 90 in the ratio of elastic scattering at 180° to that at 90° and also a peak near $A=90$ in the p-wave strength function.

Another feature of the Feshbach, Porter, and Weisskopf calculations was that broad maxima appeared in the curves of cross section vs energy; these broad maxima were identified as resonances of single partial waves of the neutron-nucleus system. Lane *et al.*[13] have extended the interpretation of neutron giant resonances in terms of single-particle resonances, explaining their great widths largely in terms of the imaginary potential of the optical model. However, there is very little correspondence between the positions of these calculated maxima and those observed experimentally (Fig. 3). A characteristic feature of each of these calculated maxima is that it shifts to *lower* energy with increasing mass number (i.e., *negative* slope in the E, $A^{\frac{1}{3}}$ plane), although Barschall[2] had noted that experimentally the maxima seemed to shift to *higher* energy with increasing mass number. The reason that the maxima in the Feshbach, Porter, and Weisskopf calculations shift toward lower energy with increasing mass number is that they are all concerned with resonances at energies below the height of the centrifugal barrier at the nuclear radius for the partial waves involved. The energy being lower than the centrifugal barrier corresponds classically to an orbit which misses the nucleus. The condition for the resonance of a given partial wave in these circumstances is that there be a characteristic number of wavelengths in the radial wave function inside the nucleus, corresponding to the condition of repeated, reinforcing, internal reflections. Therefore, as the radius (or mass) is increased, the wavelength must correspondingly increase (and energy decrease) to maintain the resonance condition. Thus the slope in the E, $A^{\frac{1}{3}}$ plane is negative for resonances at energies below the barrier. Just the opposite dependence is found for the case of resonances

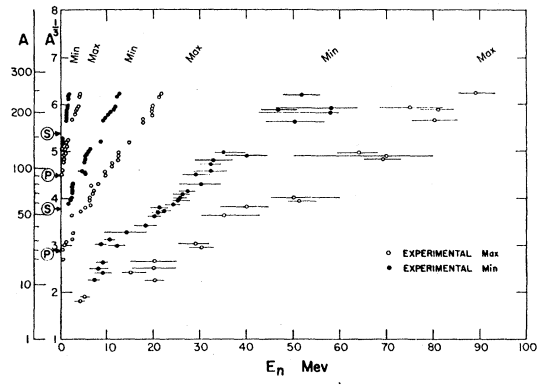

FIG. 3. Plot showing the measured positions in energy and mass number of all the known broad maxima and minima in neutron total cross sections. In addition, S and P indicate the positions of the low-energy s-wave and p-wave maxima, respectively. [The figure includes recent data from Bowen *et. al.*[8]]

[13] A. M. Lane, R. G. Thomas, and E. P. Wigner, Phys. Rev. **98**, 693 (1955): E. P. Wigner, Am. J. Phys. **23**, 371 (1955).

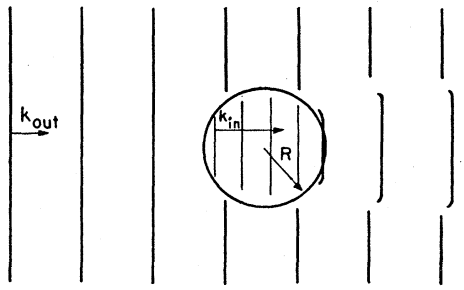

FIG. 4. Basic picture of the Ramsauer process. Neutron wave is incident on nucleus represented by a square potential well of radius R. Interference between that part of the wave which has traversed the nucleus and that part which has gone around causes oscillations in the total cross section.

at energies greater than the height of the centrifugal barrier at the nuclear radius. This case corresponds classically to an orbit which intercepts the nucleus. It is shown in Appendix I for this case that the resonance shifts to higher energy as the radius is increased, i.e., that the slope in the E, $A^{\frac{1}{3}}$ plane is positive for energies greater than the centrifugal barrier involved.

Optical-model calculations at higher energies have been more successful. The model of Bjorklund and Fernbach[14] has reproduced not only the total cross-section data in the 7- to 30-Mev region,[7] both qualitatively and quantitatively, but also the elastic scattering angular distributions[15] and the nonelastic cross sections[16] in this energy range.

The success of the optical model in general is such that there is little doubt that it can explain the measurements, in the sense that it can predict all the measured cross sections. However, the calculations generally involve many partial waves and are so complex as to require the use of an electronic computer. As a result it is not easy to get a simple interpretation or intuitive picture of the basic processes involved in these interactions. It is the purpose of this paper to point out that a simple and comprehensive interpretation of the giant resonances is afforded by the concept of a nuclear Ramsauer effect, which is analogous to the well-known electron effect.[17]

II. NUCLEAR RAMSAUER EFFECT

The following qualitative picture was suggested by Mottelson and Glassgold[18] as a means of explaining the

[14] F. Bjorklund and S. Fernbach, Phys. Rev. **109**, 1295 (1958).

[15] J. D. Anderson, C. C. Gardner, J. W. McClure, M. P. Nakada, and C. Wong, Phys. Rev. **110**, 160 (1958): **115**, 1010 (1959). Also, J. H. Coon, R. W. Davis, H. E. Felthauser, and D. B. Nicodemus, *ibid.* **111**, 250 (1958).

[16] M. H. MacGregor, W. P. Ball, and R. Booth, Phys. Rev. **108**, 726 (1957): W. P. Ball, M. H. MacGregor, and R. Booth, *ibid.* **110**, 1392 (1958): and M. H. MacGregor, W. P. Ball, and R. Booth, *ibid.* **111**, 1155 (1958). Also, T. W. Bonner and J. C. Slattery, *ibid.* **113**, 1088 (1959).

[17] C. Ramsauer, Ann. Phys. **66**, 546 (1921): N. F. Mott and H. S. W. Massey, *Theory of Atomic Collisions* (Clarendon Press, Oxford, 1950), 2nd ed., p. 206.

[18] B. R. Mottelson and A. E. Glassgold (private communications).

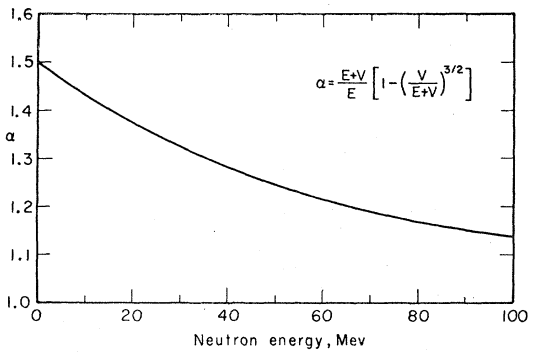

FIG. 5. Plot of α, the ratio by which the average chord through a sphere is greater than $4R/3$ due to refraction.

ridge of giant maxima observed in the total cross-section data[7] in the 7- to 30-Mev region. The essential feature is the consideration of the interference of that part of the incident neutron wave which traverses the nucleus with that part of the wave which has gone around. This picture will be recognized as the same as that used by Fernbach *et al.*[19] in 1949 to explain neutron total cross sections in the 90-Mev region. The schematic picture is indicated in Fig. 4. For simplicity we represent the nucleus as a square well of radius R. Let k_{out} and k_{in} be the respective wave numbers outside and inside the well. For the case of no refraction the average chord length through a sphere is $4R/3$. (See Appendix II.) The average phase difference Δ between the wave traversing the nucleus and that going around is

$$\Delta=\tfrac{4}{3}\alpha(k_{\text{in}}-k_{\text{out}})R, \tag{1}$$

where α is a number somewhat bigger than 1 allowing for the increased path length inside the nucleus due to refraction effects. This expression for the phase difference Δ ignores absorptive effects on the grounds that if the absorption is moderate or small, it cannot, to first order, affect the average phase of the transmitted wave and, hence, cannot influence the position of an interference maximum, although of course it directly affects its magnitude. Also, reflections from all surfaces are ignored here because in a real, diffuse-edge nucleus reflections are small and their relative importance further reduced through absorption.

The condition for maximum cross section is maximum destructive interference between the two wave components, i.e.,

$$\Delta=\tfrac{4}{3}\alpha(k_{\text{in}}-k_{\text{out}})R=n\pi, \quad n=1, 3, 5, \cdots, \text{odd}. \tag{2}$$

With n even, this same expression represents the condition for a relative minimum in the cross section. Considering Δ as a function of neutron energy E and mass number A, we see that the $\Delta=n\pi$ expression represents the equations of the loci of the maxima and minima in the E, $A^{\frac{1}{3}}$ plane. To show the dependence explicitly we substitute

$$k_{\text{out}}=(2mE/\hbar^2)^{\frac{1}{2}}=0.22E^{\frac{1}{2}} \text{ (Mev) fermi}^{-1},$$
$$k_{\text{in}}=0.22(E+V)^{\frac{1}{2}} \text{ fermi}^{-1},$$
$$R=r_0A^{\frac{1}{3}}=1.15A^{\frac{1}{3}} \text{ fermi},$$

where m is the neutron mass and V is the depth of the well (in Mev). The locus Eq. (2) can thus be written as

$$A^{\frac{1}{3}}=3n\pi/\{0.88\alpha r_0[(E+V)^{\frac{1}{2}}-E^{\frac{1}{2}}]\}. \tag{3}$$

For the factor α, we used the ratio by which the average chord is greater than $4R/3$ in a sphere whose index of refraction is $(E+V)^{\frac{1}{2}}/E^{\frac{1}{2}}$. Simple geometrical optics (see Appendix II) gives this expression as

$$\alpha=\frac{E+V}{E}\left[1-\left(\frac{V}{E+V}\right)^{\frac{3}{2}}\right]. \tag{4}$$

This expression for α is plotted in Fig. 5.

The nuclear potential V is energy dependent. The values for V used in evaluating α and in the locus equation were those found by Bjorklund and Fernbach[14] in fitting various neutron data in the 7- to 30-Mev range. These values were extrapolated to higher energies with guidance by the energy dependence of Riesenfeld and Watson.[20] The values used are plotted in Fig. 6.

The loci expressed by Eq. (3) for $n=1, 2, 3, 4, 5$, and 6 are shown as solid curves in Fig. 7, on which are plotted also the experimental points of Fig. 3.

III. DISCUSSION OF RESULTS

The fit of the loci equation to the experimental families of maxima and minima is generally quite good in spite of the crudeness of the theory. The following observations about these theoretical results can be made:

(1) Evaluation of the loci equation shows that nuclear radii and potentials are such that just three families of maxima (and minima) are possible, in agreement with

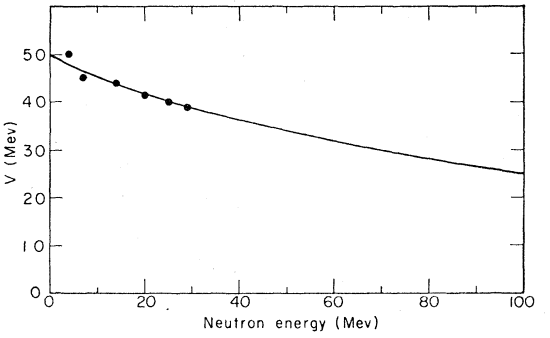

FIG. 6. The depth of the potential well used as a function of neutron energy. The values used by Bjorklund and Fernbach are shown by circles.

[19] S. Fernbach, R. Serber, and T. B. Taylor, Phys. Rev. **75**, 1352 (1949): T. Taylor, *ibid.* **92**, 831 (1953).

[20] W. B. Riesenfeld and K. M. Watson, Phys. Rev. **102**, 1157 (1956).

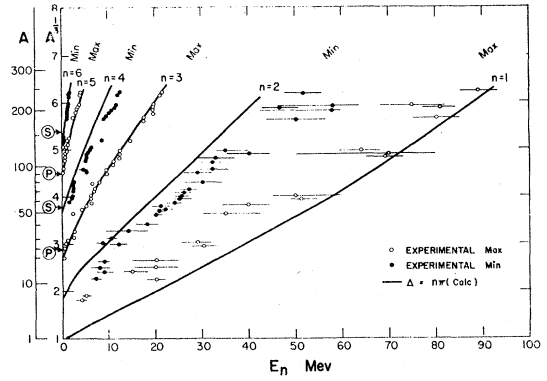

FIG. 7. Plot showing the agreement of the calculated loci of maxima and minima (solid curves) with the observed values (points) taken from Fig. 3.

observation. This neutron-nuclear situation contrasts with the electron-atomic case, in which the corresponding radii and potentials are such that only one family of Ramsauer maxima and minima are possible. In other words, near zero electron energy the radius and the well depth of the atomic potential of the noble gases are such that just one electron wavelength fits inside the atom, whereas in the corresponding neutron-nucleus case as many as three full wavelengths can fit inside the nucleus.

(2) The agreement between theory and experiment holds down to very low energies. On the one hand, this agreement at low energies is surprising because the basic picture used is one that has been expected to have validity only at relatively high energies. On the other hand, it is not completely unexpected because the loci Eq. (2) for maxima (n odd) reduces at zero energy precisely to $k_{\text{in}}R=(m+\frac{1}{2})\pi$, the condition for zero-energy s-wave resonances, which was used by Feshbach, Porter, and Weisskopf to explain the peaks in the zero-energy strength function and the scattering length distributions. The present theory calls for the zero-energy maxima to occur at the intercepts of the $n=3$ and $n=5$ families of maxima, and this is just where the p-wave maxima of Newson were found, namely at $A^{\frac{1}{3}}=2.9$ and 4.5, as shown in Fig. 7. However, the present theory calls for $k_{\text{in}}R=(m+\frac{1}{2})\pi$ $(=\frac{1}{2}n\pi$ with n odd) at this point, whereas the theory of Feshbach, Porter, and Weisskopf prescribes $k_{\text{in}}R=m\pi$. Thus there is a serious difference in the parameters of the nuclear wells which have been fitted to the data. Since at low energy only the product $k_{\text{in}}R$ occurs in the theory, one can not determine the well depth and radius separately but only the product VR^2. In the Feshbach, Porter, and Weisskopf fit to the low-energy data the product VR^2 is about $88A^{\frac{2}{3}}$ Mev fermi^2, whereas in the present fit to data which extends up to much higher energy but which also overlaps the region fitted by Feshbach, Porter, and Weisskopf a product of about $66A^{\frac{2}{3}}$ Mev fermi^2 is obtained (at low energies). This discrepancy is not understood. The present picture must fail near zero energy, for it can not explain the s-wave maxima, which occur very near the zero-energy intercepts of the $n=4$ and $n=6$ families of minima (at $A^{\frac{1}{3}}=3.8$ and 5.4, $A=55$ and 155), as shown in Fig. 7.

(3) The disagreement seen between theory and experiment for the $n=1$, 2, and 4 curves are qualitatively understandable in the following perturbation sense. The theory which has been used here can be considered as supplying a relatively small and oscillating correction or perturbation term $g(E)$ to a dominant and slowly varying unperturbed cross-section expression $F(E)$, derived from a black-nucleus model (which, we know, predicts the correct average cross section). That is, one can consider

$$\sigma_t=F(E)+g(E), \tag{5}$$

where $F(E)$ could be something like $2\pi(R+\lambda\!\!\!^{-})^2$. The loci equation derived above predicts the positions of the maxima and minima of only the correction term $g(E)$, whereas the experimental points are the corresponding extreme in the total function σ_t. As shown in Fig. 8, it is clear that the maxima of σ_t are shifted toward lower energies and the minima toward higher energies from the corresponding maxima and minima of the oscillating function $g(E)$. The amount of shift depends, of course, upon the slope $dF(E)/dE$ and upon the amplitude and wavelength of $g(E)$. In this way one can qualitatively understand the apparent theoretical-experimental discrepancies seen in the $n=1$, 2, and 4 families. (The constant r_0 was chosen originally to ensure a good fit of the theory to the experimental points along the $n=3$ family, and it must have helped the fit for the $n=5$ family. The lack of discrepancy along the $n=6$ family is probably due to the smallness of the inherent shift here, as the amplitude of the oscillating function is relatively large and its wavelength along the energy scale relatively small. A slight adjustment of the constants of the theory would be adequate to give a better over-all fit with the experimental points, i.e., a fit that is more equitable among the 6 families; the lack of this improvement is attributable to personal inertia.)

These relative shifts and the magnitudes of the oscillations can be used to evaluate roughly the amount of nuclear absorption. However, since the purpose of this rough treatment is merely to give a qualitative picture of the processes involved and since a much better evaluation can easily be done with a complete optical-

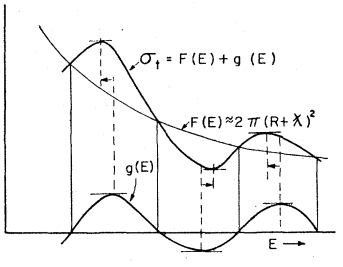

FIG. 8. Schematic graph demonstrating relative shifts in the maxima and the minima of the total function σ_t from those of the oscillating function $g(E)$.

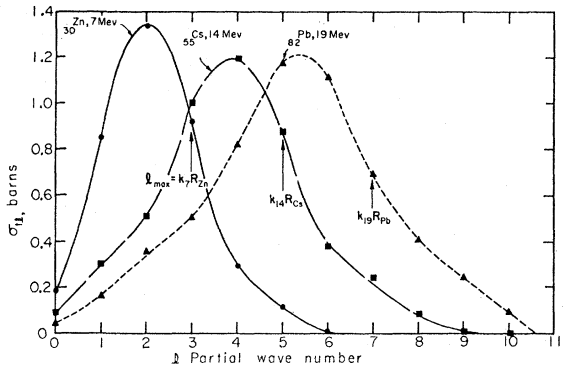

FIG. 9. The distributions in l of the partial wave contributions to the total cross section for three cases lying on the $n=3$ family of broad maxima. The values were obtained from exact calculations on the complete optical model of Bjorklund and Fernbach.

model calculation, it does not seem profitable to carry this theory very far in that direction.

Since in Eq. (3) the quantities V and R are mathematically separated, it was hoped by fitting all the loci of maxima and minima that each quantity could be separately determined rather than just the familiar product VR^2. Although in principle this separate determination is possible, the hope was in vain, for approximately equally good fits are obtained if one varies V by, say, 20% but holds the product VR^2 constant.

IV. COMPARISON WITH EXACT CALCULATIONS

The question as to why this simple picture works so well was explored in the following way. The details of some successful, exact optical-model calculations were examined to see the behavior of the various partial waves involved. These calculations were very kindly provided by Bjorklund. In particular, the contribution of each partial wave to the total cross section at three representative points along the $n=3$ family of maxima of Fig. 7 were evaluated. These points were: zinc at 7 Mev, cesium at 14 Mev, and lead at 19 Mev. The partial wave contributions[21] to these total cross sections are shown in Fig. 9. This plot shows that the identity of the partial waves which contribute most to the total cross section varies smoothly and rapidly as one travels along a continuous family of maxima. In each of the three cases the largest l value of importance is equal to $k_{\text{out}}R$ (the largest l value classically possible), and the l value at the maximum is equal to $(k_{\text{out}}R-1)$.

These exact optical-model calculations plotted in Fig. 9 show not only that the partial wave population changes widely as you traverse a continuous family of broad maxima, but also that at any point many partial waves are generally important. To see this point more clearly, consider the phase shifts involved, as follows: The general expression for the total cross section in terms of a set of complex phase shifts δ_l is

$$\sigma_t \equiv \sum_{l=0} \sigma_{tl} = \frac{4\pi}{k_{\text{out}}^2} \sum_{l=0} (2l+1) b_l, \tag{6}$$

where $b_l \equiv$ imaginary part of $\exp(i\delta_l)\sin\delta_l$. Let $\delta_l \equiv \alpha_l + i\beta_l$. Then

$$b_l = \tfrac{1}{2}(1-e^{-2\beta_l}\cos 2\alpha_l).$$

In the limit of zero nuclear absorption, $\beta_l=0$ and $b_l=\sin^2\delta_l$, which is a more familiar expression for the phase factor. Thus, dividing each value σ_{tl} in Fig. 9 by $4\pi(2l+1)/k_{\text{out}}^2$, we get the plot of the phase factor b_l shown in Fig. 10. This plot shows that *all* the partial waves from $l=0$ to $l_{\max}=k_{\text{out}}R$ have important and comparable phase shifts.

This phase factor plot, which was obtained from exact calculations of a full-blown optical model, serves to justify the simple wave picture from which the $\Delta(A,E)=n\pi$ equation was derived, for the basic statement of the simple picture is that it is the over-all or average phase shift of all of the wave front classically intercepted by the nucleus which must be considered, i.e., that many partial waves are simultaneously important. Furthermore, the phase factor distribution of Fig. 10 corresponds in detail very well with the distribution one would obtain using the simple picture (with absorption) and considering the lth partial wave as an annular section of the incident wave front whose inner and outer radii are $l\lambda$ and $(l+1)\lambda$, respectively. This picture was justified also by Fernbach *et al.*[19] in their 90-Mev work by means of a WKB analysis.

V. CONCLUSIONS

In summary, we have seen that the several families of neutron giant resonances observed in the neutron total cross sections can be simply understood as maxima created by interference between that part of the neutron wave which has traversed a partially transparent nucleus and that part which has gone around it. Each family can be simply characterized by the relative phase shift of $n\pi$ between the two wave components. An alternative interpretation of these maxima as resonances of single partial waves is not satisfactory because in general at any maximum several partial waves are simultaneously important; furthermore, the partial wave distribution

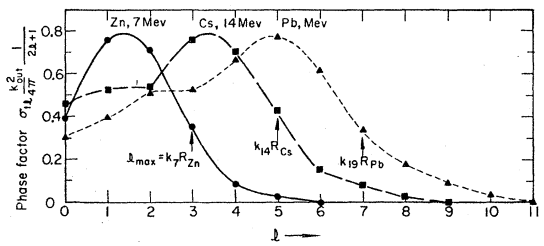

FIG. 10. Plots of the phase factors corresponding to the partial wave cross-section contributions of Fig. 9.

[21] The calculations were performed using spin-dependent potentials. For simplicity of presentation in Fig. 9 the spin-up and spin-down contributions were lumped together for each partial wave.

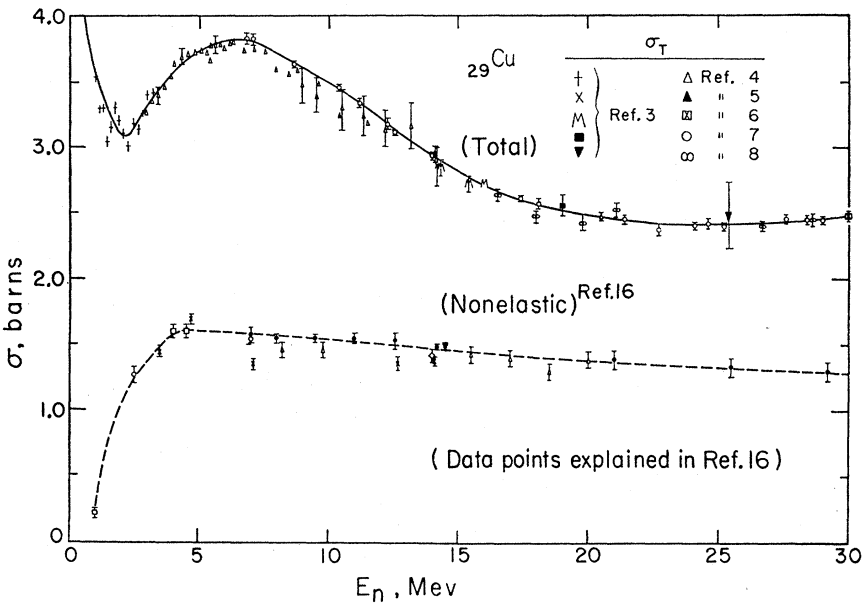

FIG. 11. The measured neutron total and nonelastic cross sections for copper as functions of energy.

changes markedly as one moves along a continuous family of maxima.

Another point coming from this interpretation of the neutron giant resonances concerns their widths, which are found to be of the same order as their spacings. This fact is understandable from the viewpoint that the incident neutron makes but one pass through the nucleus, so that as you move in energy from one maximum to the next, the cross section can change only very slowly and gently—like a sinusoid. That is, the condition of repeated, reinforcing, internal reflections, which is necessary for a resonance narrow relative to the spacing between resonances, is missing here. The widths of the giant resonances are, therefore, of the same order of magnitude as the spacings and thus are related more to the nuclear size and the real potential than to the imaginary potential. A supporting argument for the absence of appreciable internal reflections comes from considerations of the nonelastic cross section. If the nonelastic cross section depended in any way upon interference effects, then it too would exhibit structure. However, no structure at all is apparent in the experimental data (nor does it appear in the optical-model predictions) at energies much greater than the thresholds for inelastic scattering. Typical plots of both total and nonelastic[16] cross sections versus energy are shown in Figs. 11–13. It can be seen that there is no structure in the nonelastic cross sections which corresponds to the very pronounced structure in the total cross sections. It is also interesting to see these cross sections plotted as functions of mass number. In Fig. 14 (obtained from Ball *et al.*[16]) total and nonelastic cross sections measured at 14 Mev, normalized by $\pi(R+\lambda\!\!\!^{-})^2$, are plotted vs $A^{\frac{1}{3}}$. The nonelastic cross sections are consistently equal simply to 1.0 times geometrical, while the total cross sections oscillate smoothly about 2.0 times geometrical. The dashed curve is the difference between the total and non-elastic plots and shows explicitly that the elastic cross section contains all the structure. This behavior is just what is called for on the basis of the one-pass picture.

VI. CONCLUDING REMARKS

I have found that this nuclear Ramsauer picture has been used before. Lawson[22] similarly derived an equation for the locus of the maxima and used it to interpret the high-energy (30 to 150 Mev) data of Taylor and

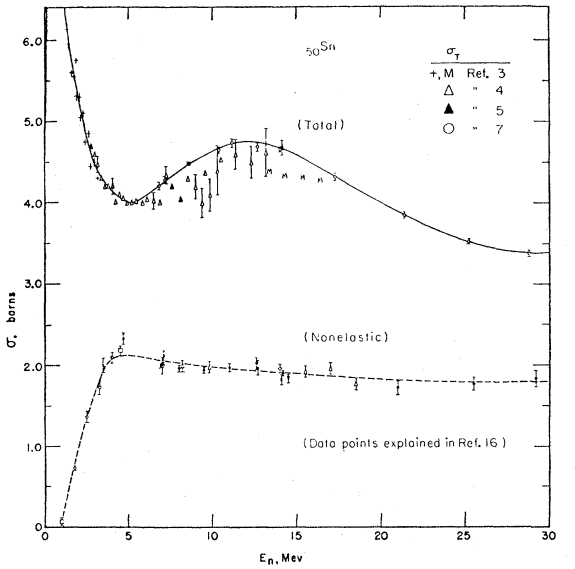

FIG. 12. The measured neutron total and nonelastic cross sections for tin as functions of energy.

[22] J. D. Lawson, Phil. Mag. 44, 102 (1953).

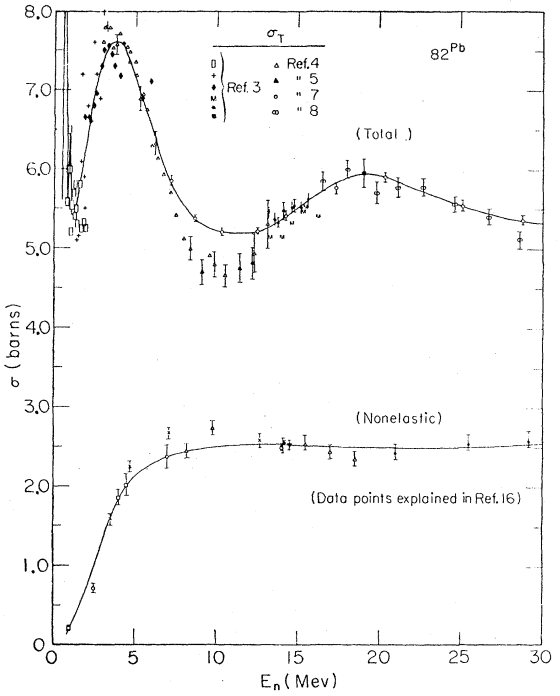

FIG. 13. The measured neutron total and nonelastic cross sections for lead as functions of energy.

Wood.[6] He noted that the formula predicted other maxima at lower energies but doubted that his considerations were valid at such energies. Carpenter and Wilson also refer to the high-energy resonances as "akin to a nuclear Ramsauer effect."[23] Nemirovski's work too contains many of the features mentioned here.[24] Although many features of the broad maxima have been noted before in various places, the general simple systematics of the whole ensemble have not previously been realized. An early report on this work was given in 1960.[25]

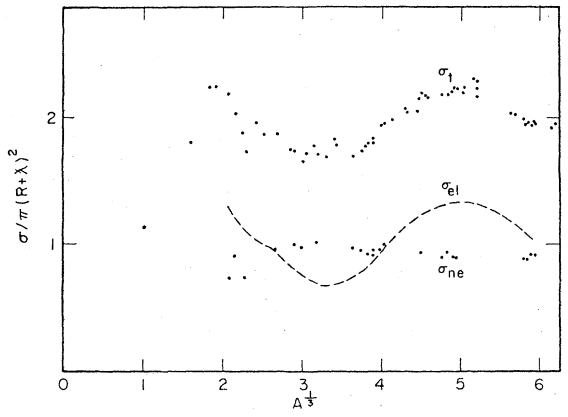

FIG. 14. The measured 14-Mev neutron total (upper points) and non-elastic (lower points) cross sections divided by $\pi(R+\lambda)^2$ as functions of $A^{\frac{1}{3}}$. R here was taken equal to $(1.26A^{\frac{1}{3}}+0.75)$ fermis (reference 16). The dashed curve represents the elastic cross section: it is the difference between the upper and lower sets of points. [See M. H. MacGregor, W. P. Ball, and R. Booth, Phys. Rev. **108**, 726 (1957).]

ACKNOWLEDGMENTS

I am grateful to B. R. Mottelson and A. Glassgold for first suggesting the basic picture involved, to F. Bjorklund for the optical-model calculations, to J. P. Stoering for much data processing and many calculations, and to B. R. Mottelson, E. Teller, P. C. Gugelot, and many others for helpful criticism and discussion.

APPENDIX I: PROOF THAT A RESONANCE SHIFTS TO HIGHER ENERGY WITH INCREASING NUCLEAR SIZE FOR ENERGIES GREATER THAN THE CENTRIFUGAL BARRIER

Consider a neutron of energy E (and wave number k) incident on a nucleus A. The neutron-nucleus interaction is represented by an attractive potential well $V_n(r)$, whose exact shape need not be specified except that it have a reasonably well-defined radius $R=r_0A^{\frac{1}{3}}$. We consider a case such that the lth partial wave is in resonance, where $l<kR$, i.e., the lth phase shift $\delta_l=\pi/2$ and $E>V_l(R)$, $V_l(r)=\hbar^2l(l+1)/2mr^2$ being the centrifugal potential associated with the lth partial wave. This situation is illustrated in Figs. 15(a) and (b), where $u(r)$

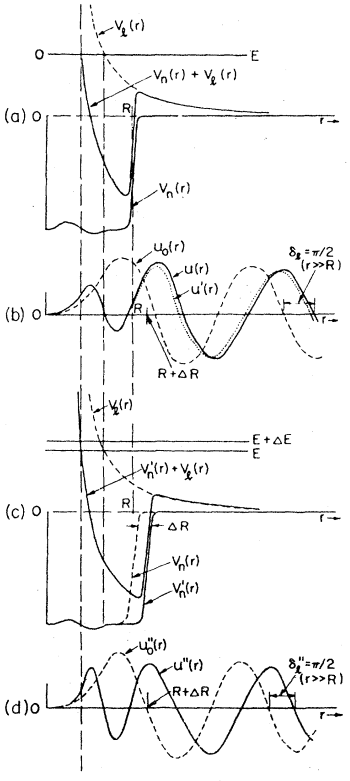

FIG. 15. Figures illustrating the proof that a resonance of the lth partial wave, for $l<kR$, shifts to higher energy with increasing mass number. $V_n(r)$ is the nuclear potential well. $V_l(r)$ is the centrifugal potential corresponding to the lth partial wave. $u_0(r)$ is the radial wave function at energy E for the lth wave in the absence of $V_n(r)$. $u(r)$ is the corresponding function with $V_n(r)$ present and represents a resonance condition. $u(r)$ is changed to $u'(r)$ (off resonance) by the increase in nuclear radius ΔR. $u_0''(r)$ and $u''(r)$ represent the new resonance situation brought about by a compensating increase in energy ΔE.

[23] S. G. Carpenter and R. Wilson, Phys. Rev. **114**, 510 (1959).
[24] P. E. Nemirovski, *Proceedings of the International Conference on the Peaceful Uses of Atomic Energy, Geneva, 1955* (United Nations, New York, 1956), Vol. 2, p. 86.
[25] J. M. Peterson, Bull. Am. Phys. Soc. 5, 32 (1960).

and $u_0(r)$ are the radial functions (times r) of the lth partial wave of energy E with and without the presence of the nuclear potential $V_n(r)$, respectively. $u_0(r)$ is the spherical Bessel function $j_l(kr)$ (times r) and has its first peak just beyond $kr=l$. The phase shift δ_l is defined as the phase difference between $u_0(r)$ and $u(r)$ for $r\gg R$.

Now consider the effects on the wave functions produced by a small increase ΔR of the nuclear radius, illustrated in Figs. 15(b) and (c). $u_0(r)$, being independent of $V_n(r)$, is unchanged; also $u(r)$ for $r<R$ is unchanged, for in this region $V_n(r)$ is unchanged. However, for $r>R$, $u(r)$ has been changed to $u'(r)$, all of whose characteristic points have been shifted to slightly smaller radii because of the increased curvature of the wave function in the region ΔR. The system is now slightly off resonance.

Next we consider how the energy is to be changed in order that the phase shift be returned to $\pi/2$. Consider the energy dependence of the functions $u'(r)$ and $u_0(r)$. As the energy increases, the wavelength decreases, and all of the characteristic points of each function shift to smaller radii. However, the two functions shift at different rates. A characteristic point of $u'(r)$ shifts more slowly with energy than a corresponding point of $u_0(r)$, because for $r<(R+\Delta R)$ the effective wavelength of $u'(r)$ [corresponding to an effective kinetic energy $E_k=E-V_n(r)-V_l(r)$] is everywhere smaller than that of $u_0(r)$ [whose wavelength corresponds to the smaller effective kinetic energy $E-V_l(r)$]. For $r>R$, the wavelengths of $u'(r)$ and $u_0(r)$ are, of course, everywhere the same. Since the change in wavelength $\Delta\lambda\!\!\!^{-}$ due to a shift in energy ΔE is $\Delta\lambda\!\!\!^{-}=-\lambda\!\!\!^{-}\Delta E/2E_k$, it is thus clear that a maximum in $u'(r)$ will not shift as much as a corresponding maximum in $u_0(r)$. In other words, because of the effect of the nuclear potential $V_n(r)$ the phase of the wave function $u'(r)$ for $r<R$ is relatively stable to an incremental change in energy when compared to that of the function $u_0(r)$. Thus since the phase of $u_0(r)$ changes faster with energy than that of $u'(r)$, we see that there is a positive ΔE such that the phase shift δ_l will be returned to $\pi/2$, as illustrated in Fig. 15(d), where $u''(r)$ and $u_0''(r)$ are the analog of $u'(r)$ and $u_0(r)$, respectively, for the energy $E+\Delta E$.

This argument applied in the opposite direction shows for a negative ΔE that the phase shift goes further from $\pi/2$. Thus the slope $dA^{\frac{1}{3}}/dE$ of a resonance locus in the $A^{\frac{1}{3}}, E$ plane is positive for any partial wave if $E>V_l(R)$. This energy condition, which is equivalent to $l<kR$, corresponds classically to the condition that the classical orbit intercepts the nucleus. For the particular case of s waves, our result shows that the slope of the locus is positive for *all* positive energies.

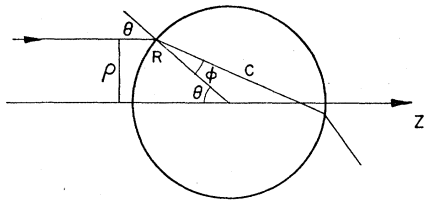

FIG. 16. Ray geometry.

APPENDIX II. AVERAGE CHORD LENGTH THROUGH A SPHERE

We wish to derive the average chord length through an evenly illuminated sphere of radius R and index of refraction n. Let the z axis be parallel the radiation and go through the center of the sphere. Consider a ray incident at radius ρ from the z axis (Fig. 16). Its chord length, C, is $2R\cos\varphi$, φ being the angle of refraction and θ the angle of incidence. Snell's law relates the angles and the index of refraction as $\sin\theta/\sin\varphi=n$. The average chord length $\bar{C}$ for uniform illumination in the z direction is

$$\bar{C}=\frac{1}{\pi R^2}\int_0^R C2\pi\rho d\rho.$$

Let $\rho=R\sin\theta$. Then

$$\bar{C}=4R\int_0^1 \cos\varphi\,\sin\theta d\,\sin\theta$$

$$=4Rn^2\int_0^{\sin^{-1}(1/n)} \cos^2\varphi\,\sin\varphi d\varphi.$$

$$\bar{C}=\frac{4R}{3}n^2\left[1-\left(1-\frac{1}{n^2}\right)^{\frac{3}{2}}\right],$$

which reduces to $\bar{C}=4R/3$ for $n=1$ (no refractive effects) and gives Eq. (4) for $\alpha=\bar{C}/(4R/3)$ and $n=(E+V)^{\frac{1}{3}}/E^{\frac{1}{3}}$.